

# Simulating quantum chemistry in the restricted Hartree-Fock space on a qubit-based quantum computing device

Vincent E. Elfving,<sup>1</sup> José A. Gámez,<sup>2</sup> and Christian Gogolin<sup>2</sup>

<sup>1</sup>*Qu & Co B.V., Palestrinastraat 12H, 1071 LE Amsterdam, The Netherlands*

<sup>2</sup>*Covestro Deutschland AG, 51365 Leverkusen, Germany*

(Dated: March 29, 2022)

Accurate quantum chemistry simulations remain challenging on classical computers for problems of industrially relevant sizes and there is reason for hope that quantum computing may help push the boundaries of what is technically feasible. While variational quantum eigensolver (VQE) algorithms may already turn noisy intermediate scale quantum (NISQ) devices into useful machines, one has to make all efforts to use the scarce quantum resources as efficiently as possible. We combine the so-called restricted approximation from computational quantum chemistry with techniques for simulating molecular chemistry on gate-based quantum computers and thereby obtain a much more resource efficient algorithm with little accuracy loss. In fact, we show that using the quantum resources freed up by means of the restricted approximation for increasing the basis set can lead to more accurate results and reductions in the necessary number of quantum computing runs (shots) by several orders of magnitude, already for a simple system such as lithium hydride.

## I. INTRODUCTION & BACKGROUND

One of the most promising near term applications of quantum computers is in the simulation of quantum Hamiltonians in quantum chemistry. Current classical algorithms for accurately simulating the behavior of molecules are very computationally costly or simply prohibited. These can be classified into two main categories: based on the electronic wavefunction of the molecular system or on their electronic density. In the latter, known as density functional theory (DFT), the accuracy of the results depends on the system investigated and requires a prior assessment, which prevents them from being universally applicable. Among the wave function based methods, two are noteworthy because of their universally high accuracy: Full-Configuration Interaction (FCI) and Coupled Cluster (CC) techniques. The FCI solution to an electronic structure Hamiltonian is numerically exact but requires exponential time on a classical computer, limiting its applicability to systems with few atoms and/or electrons. Within the CC techniques, the CCSD or particularly CCSD(T), considered the ‘golden standard’ of computational chemistry, are noteworthy; they have resource requirements scaling as  $\mathcal{O}(N^6)$  or  $\mathcal{O}(N^7)$  respectively, where  $N$  is the number of orbitals in the problem. This limits their applicability to very small chemical problems with little industrial interest.

The very high computational complexity of simulating chemistry on a computer has spurred a large interest in simulating quantum chemistry on a quantum processor. The idea of using quantum systems, like quantum computers, to describe quantum systems, like chemical molecules, dates back to the 1980s [1]. Indeed comparably few, on the order of  $10^2$ , qubits could be sufficient to demonstrate a practical quantum advantage in this area while the largest commercially available gate-based quantum computer today already has 53 qubits [2]. We refer to Ref. [3] for an extensive overview on the application of quantum computers to chemistry. In short, state-of-the-art algorithms for simulating chemistry on a quantum computer can be roughly categorized into near-term NISQ (Noisy Intermediate Scale Quantum [4]) compatible and future FTQC

(Fault Tolerant Quantum Computing) algorithms. Simulating ground state energies on a FTQC can be done with a variety of algorithms, where (various variants of) the Quantum Phase Estimation (QPE [5, 6]) algorithms are a principal candidate. QPE may in principle simulate spectra and dynamics of chemistry Hamiltonians to arbitrary accuracy; however, the coherence requirements are much more stringent than present-day quantum devices allow for.

Conversely, in the NISQ era, the most widely used algorithm for ground-state estimation is the Unitary Coupled Cluster with Single and Double excitations Variational Quantum Eigensolver (UCCSD-VQE) [7]. UCCSD-VQE is a variational technique in which a state approximate to the ground state is prepared first, such as a Hartree-Fock state, after which a suitable ansatz is applied to it in a variational hybrid quantum-classical approach in order to improve over the initial ansatz and prepare a better approximation of the true ground state. The UCCSD method can be seen as a unitary analog to the classical-computational chemistry CCSD protocol [8], and is expected to give comparable accuracy.

Using a Gaussian orbital basis decomposition of the wavefunction with a Hamiltonian expressed in second-quantization, the quantum circuit depth scaling of the UCCSD protocol is  $\mathcal{O}(N^4)$  in state-of-the-art algorithm proposals [9], where the number of measurements has a pre-factor scaling between  $\mathcal{O}(N^3)$  and  $\mathcal{O}(N^4)$  due to the number of non-commuting Hamiltonian terms. Using a particular dual to a plane-wave basis decomposition for the Hamiltonian [10] in combination with a fermionic swap-network [11] allows for implementing Trotterized operator evolution on a linear array of qubits with depth scaling  $\mathcal{O}(N)$ , and number of required terms to perform tomography scaling as  $\mathcal{O}(N^2)$ . However, a periodic basis set may be ill-suited for simulating molecular chemistry; the construction of pseudo-potentials analogous to those in conventional plane-wave decompositions is not proposed yet; and a chemistry-inspired quantum ansatz in a periodic basis set has of yet not been identified. In a related work, Ref. [12], also a linear-depth method was proposed. Although that work naturally enables systematic improvements

through the parameter  $k$ , in that work the singlet-state restriction was not applied explicitly to the Hamiltonian mapping as we do in this work, which means a factor two difference in qubit number requirements of the respective mappings (which has implications for the basis set size or number of included orbitals), in addition to the Hamiltonian measurement of the energy being vastly simplified in the method presented here.

Given the constraints of NISQ devices it is highly desirable to further reduce the quantum resource requirements of UCC-based variational algorithms. Taking the ideas developed in classical computational chemistry seriously and translating them to the quantum world can be a good guiding principle. In this paper, we present an efficient quantum algorithm for preparing eigenstate wavefunctions and energies of molecular systems, using the well known restricted approximation, in which electrons are modeled as singlet pairs rather than individual fermions. In this approximate mapping, the simulation can be executed with a two-fold increase in simulable system size or basis set, using the same quantum hardware resources. The implementation of this mapping on a quantum computer is combined with a novel restricted unitary coupled cluster ansatz with an efficient Trotter step circuit decomposition, in order to simulate molecular chemistry with a circuit gate depth reduction from  $\mathcal{O}(N^4)$  to  $\mathcal{O}(N)$  as compared to state-of-the-art unitary coupled cluster techniques. We here concentrate on variational algorithms for near-term quantum computers, although the mapping and ansatz are also well-suited for future FTQC devices. The reduction in accuracy as compared to a non-restricted Hilbert space can be observed as a trade-off with the gate depth and qubit number requirements; we show how the mapping potentially allows for increased accuracy given a fixed set of available qubits, where we simulate the groundstate of the lithium hydride molecule in a variational-version implementation example. Finally, we show how the proposed variational method also presents a faster convergence by several orders of magnitude with respect to the total number of quantum circuit calls than conventional UCCSD-VQE.

## II. HAMILTONIANS IN COMPUTATIONAL CHEMISTRY

To turn a chemical problem into a well defined computational problem one routinely makes a series of assumptions and approximations. The first standard assumption is the Born-Oppenheimer approximation, which decouples the nuclear and electronic degrees of freedom. Considering that electrons move much faster than nuclei in molecules, the Born-Oppenheimer approximation consider the latter as frozen point charges in space. One is then faced with an electronic structure problem, i.e., the problem of determining the behavior of the electrons of the system in the potential created by the nuclei and the background. For an introduction to the electronic structure problem, and a description of classical and quantum algorithms which solves these problems, we refer the reader to Refs. [3, 13]. All wave function based methods require a discretization of the electronic structure problem, which a priori is a continuum problem of electrons in

three dimensional space.

In the standard approach one decides to model the electrons of the system individually and introduces a finite set of basis functions (a so-called basis set) to discretize the problem and thereby make it amenable to a solution on a digital computer. Each basis function is taken to represent a fermionic mode.

The resulting many-body Hamiltonian, acting on the fock space over these modes can then be written in second quantized form as follows [3]

$$\hat{H} = C + \sum_{p,q} h_{p,q} \hat{a}_p^\dagger \hat{a}_q + \frac{1}{2} \sum_{p,q,r,s} h_{p,q,r,s} \hat{a}_p^\dagger \hat{a}_q^\dagger \hat{a}_r \hat{a}_s, \quad (1)$$

where  $C$  is a constant energy offset,  $\{p, q, r, s\}$  are fermionic mode indices,  $\hat{a}_p$  is the fermionic annihilation operator of the  $p$ -th fermionic mode, and  $h_{p,q}$  and  $h_{p,q,r,s}$  are Hamiltonian matrix elements which are determined by means of integrals involving the basis functions and potentials of the nuclei, for example using Hartree-Fock theory or self-consistent-field methods [14] (see Appendix A for details). The number of terms in this Hamiltonian is  $\mathcal{O}(N^4)$ , where  $N$  is the number of orbitals.

The number of fermionic modes and the values of the matrix elements depend on the choice of basis set. For example, in a minimal basis set, like the STO-6G basis, as many basis functions are used as core and valence orbitals of the molecule under study. In the case of the lithium hydride (LiH) molecule we consider as an example in this paper, the number of basis functions is 6. Electrons being spin-1/2 particles, two of them can occupy a single fermionic mode (spin-up and spin-down). This brings the total number of spin-orbitals (SOs) to 12.

The fermionic Hamiltonian in Eq. (1) can be mapped to qubits on a gate-based quantum computer with the help of a variety of transformations (such as the Jordan-Wigner transformation [15]). The result of this is a Hamiltonian consisting of a sum of Pauli string operators, i.e., tensor products of the Pauli operators  $\hat{\sigma}^X$ ,  $\hat{\sigma}^Y$ , and  $\hat{\sigma}^Z$  and the  $2 \times 2$  identity operator.

## III. DISCRETIZATION IN THE RESTRICTED APPROXIMATION

In this work, we employ the restricted Hartree-Fock approximation [8] during the discretization step. This approximation effectively restricts the problem to a subspace of the full Hilbert space of all possible many-body electronic states that is spanned by those states in which orbitals are either empty or occupied by an electron singlet pair (because of the Pauli exclusion principle). The restricted ansatz is rather widespread in computational chemistry and has proved to deliver sufficient accuracy for the description of chemical systems. Indeed its usage has become standard in computational chemistry [16]. This is so, as quite often in molecular systems all the electrons are distributed in electronic pairs occupying the same spacial orbital.

The Hamiltonian can then be written as

$$\hat{H}_r = C + \sum_{p,q} h_{p,q}^{(r1)} \hat{b}_p^\dagger \hat{b}_q + \sum_{p \neq q} h_{p,q}^{(r2)} \hat{b}_p^\dagger \hat{b}_p \hat{b}_q^\dagger \hat{b}_q, \quad (2)$$

where  $\hat{b}_p$  represents the electron-pair annihilation operator in mode  $p$ , where each mode is limited to either 0 or 1 excitation. The matrix elements  $h_{p,q}^{(r1)}$  and  $h_{p,q}^{(r2)}$  are related to the single- and two-electron integrals (see A for details). This operator can be defined via the hard-core boson (HCB) (anti-)commutation relations [17]

$$[\hat{b}_p, \hat{b}_q^\dagger] = [\hat{b}_p^\dagger, \hat{b}_q^\dagger] = [\hat{b}_p, \hat{b}_q] = 0 \quad (p \neq q) \quad (3)$$

$$\{\hat{b}_p^\dagger, \hat{b}_p^\dagger\} = \{\hat{b}_p, \hat{b}_p\} = 0 \quad (4)$$

$$\{\hat{b}_p, \hat{b}_p^\dagger\} = 1 \quad (5)$$

The connection here is that a singlet pair of electrons has even spin and thus behaves like a boson, while no more than 2 electrons can occupy the molecular orbitals at once. Notice that this Hamiltonian is far simpler than the unrestricted fermionic Hamiltonian in (1), but still non-trivial, as it is not quadratic in the creation and annihilation operators.

As a first consequence of using the restricted approximation, the number of qubits needed to represent a given problem is halved compared with the unrestricted mapping. In the LiH example the 6 basis functions in the STO-6G basis map to 6 qubits instead of the usual 12. Alternatively, one may use the same qubit number with a larger basis set (this can be advantageous as we will show later). For example, in the 4-31G basis set, 11 molecular orbitals (MOs) result in 22 fermionic orbitals but only 11 qubits are needed in the restricted approach. In this way, with 12 qubits as a quantum resource, one may either simulate LiH in unrestricted STO-6G or in restricted 4-31G.

As the electron pair creation and annihilation operators commute, the above Hamiltonian can be mapped directly to Pauli spin operators resulting in operations native on qubit based gate quantum computer using the representation

$$\hat{b}_p = \hat{\sigma}_p^- = \frac{1}{2}(\hat{\sigma}_p^X - i\hat{\sigma}_p^Y), \quad (6)$$

where  $\hat{\sigma}_p^X$  and  $\hat{\sigma}_p^Y$  are Pauli-X and Y spin operators respectively [18].

Due to hermiticity of Eq. (2), some terms vanish, and the total qubit Hamiltonian can be written as

$$\hat{H}_{qb} = C + \sum_p \frac{h_p^{(r1)}}{2} (\hat{I}_p - \hat{\sigma}_p^Z) \quad (7)$$

$$+ \sum_{p \neq q} \frac{h_{p,q}^{(r1)}}{4} (\hat{\sigma}_p^X \hat{\sigma}_q^X + \hat{\sigma}_p^Y \hat{\sigma}_q^Y) \quad (8)$$

$$+ \sum_{p \neq q} \frac{h_{p,q}^{(r2)}}{4} (\hat{I}_p - \hat{\sigma}_p^Z - \hat{\sigma}_q^Z + \hat{\sigma}_p^Z \hat{\sigma}_q^Z) \quad (9)$$

where  $\hat{\sigma}_p^Z$  and  $\hat{I}_p$  are Pauli-Z and identity spin operators respectively.

As is apparent from both Eq. (2) and Eq. (7), the total number of local terms in the restricted Hamiltonian scales as  $\mathcal{O}(N^2)$  (as opposed to  $\mathcal{O}(N^4)$  in the unrestricted case). This, together with the fact that the Hamiltonian in Eq. (7) naturally decomposes into just two non-commuting components,

greatly simplifies the measurement of the energy in VQE schemes based on Hamiltonian averaging. In fact, the Hamiltonian terms can be grouped into just three unique tensor product bases constructible with single-qubit rotations alone.

#### IV. TRIAL STATE

A first step of both VQE and QPE algorithms, and most Hamiltonian simulation algorithms in general, is the preparation of a trial state. The success of an algorithm for determining eigenenergies of the Hamiltonian depends on the quality of the state preparation and its closeness to the actual eigenstate of interest. A good initial trial state for the groundstate of  $\hat{H}_r$  is the Hartree-Fock state, which in this case is just a product state with the  $n_e$  lowest-energy MOs occupied with a single pair of electrons. For systems with even number of electrons, the HF state in the restricted approximation is the same state as without the approximation, and the energy expectation is equal too.

Such a simple trial virtually never captures the complexity of the true, partially entangled ground state. Therefore, after preparing the HF-state on a qubit lattice, an additional circuit can be applied to the array which prepares a more general ansatz including higher-order correlators. In principle, an eigenstate of the many-body Hamiltonian could contain many complicated correlations, which implies that a large number of entangling operations need to be applied to the HF state (which is by itself a mere product state) in order to produce this highly entangled state. In practice however, single/double/triple single-particle excitations are often enough to bring the HF state sufficient close to the ground state. This idea is behind the coupled-cluster method, where typically single/double(triple) (CCSD(T)) excitations are considered.

In classical computational chemistry, a non-unitary Coupled Cluster operator is applied to the HF state as an approximation, because the unitary matrix exponential is very costly to compute. However, on a quantum computer the unitary evolution over a coupled-cluster operator can be naturally implemented. In conventional UCCSD methods the unitary operator is constructed as follows [19]:

$$\hat{U} = \exp(\hat{T}_1 + \hat{T}_{2,1} + \hat{T}_{2,2}) \quad (10)$$

$$\hat{T}_1 = \sum_{i \in v, j \in o} t_{i,j}^{(1)} (\hat{a}_i^\dagger \hat{a}_j - \hat{a}_j^\dagger \hat{a}_i) \quad (11)$$

$$\hat{T}_{2,1} = \sum_{i \in v, j \in o} t_{i,j}^{(2,1)} (\hat{a}_i^\dagger \hat{a}_j \hat{a}_{i+1}^\dagger \hat{a}_{j+1} - \hat{a}_j^\dagger \hat{a}_i \hat{a}_{j+1}^\dagger \hat{a}_{i+1}) \quad (12)$$

$$\hat{T}_{2,2} = \sum_{(p,q) \in v, (r,s) \in o} t_{p,q,r,s}^{(2,2)} (\hat{a}_p^\dagger \hat{a}_q \hat{a}_r^\dagger \hat{a}_s - \hat{a}_q^\dagger \hat{a}_p \hat{a}_s^\dagger \hat{a}_r) \quad (13)$$

where  $\{i, j\}$  and  $\{p, q, r, s\}$  are single- and two-particle fermionic mode indices respectively,  $\{v, o\}$  are the sets of virtual and occupied orbitals respectively,  $\hat{a}_p$  is the fermionic annihilation operator of the  $p$ 'th fermionic mode,  $t_{i,j}^{(1)}$  refers to excitations involving two orbitals and a single electron,  $t_{i,j}^{(2,1)}$  refers to excitations involving two distinct orbitals and two

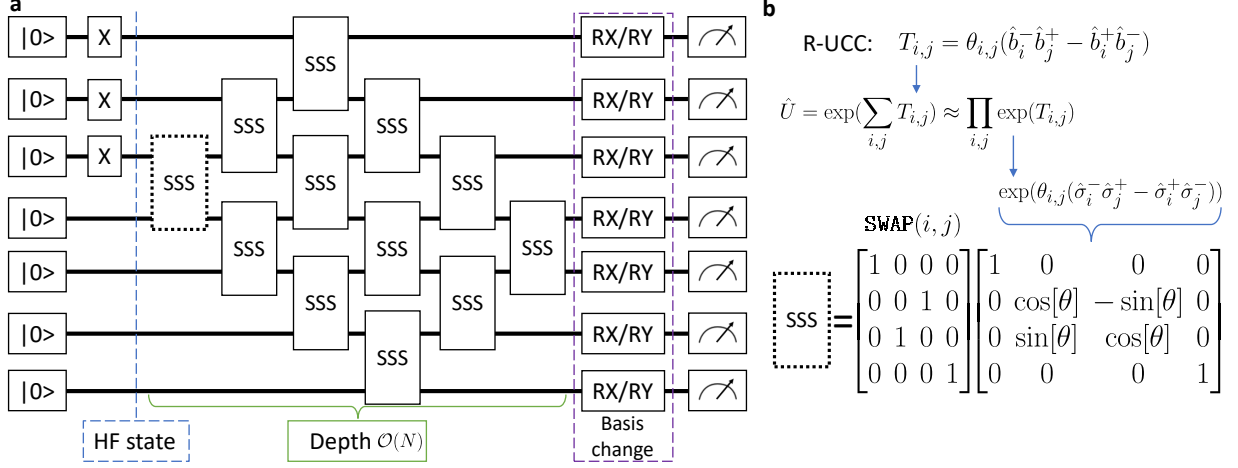


FIG. 1. **a** Quantum circuit diagram implementing a single Trotter step of the R-UCC ansatz. The qubit register is first prepared in the HF state by the application of X gates to the first  $n_e$  qubits. The R-UCC ansatz Trotter step is then implemented as a sequence of Singlet-State Simulation (SSS) gates in linear circuit depth. In a VQE implementation, the energy is estimated by Hamiltonian averaging, which is performed by rotating all the qubits to the relevant basis for those Hamiltonian Pauli-terms and measuring the qubits in their Z-basis. **b** The SSS gate is shown as a mathematical representation, and the origins from the R-UCC coupled cluster operators is detailed. The SSS gate is a combination of a partial swap gate followed by a full swap gate.

electrons, and  $t_{p,q,r,s}^{(2,2)}$  refers to excitations involving up to four distinct orbitals and two electrons.

To simulate unitary evolution operator Eq. (10) with a quantum circuit based on single and two-qubit gates (for this universality see, e.g., Ref. [20]), one can Trotterize [21] the evolution and apply each term sequentially or in a structured way [22, 23]. If the amplitudes are not too big, this Trotterization leads only to small errors with the true UCCSD state. Often a single Trotter step can be sufficient to accurately and efficiently reproduce the ground-state energy of simple molecular systems [24] and the robustness inherent to VQE may even partially compensate the Trotter errors [25].

Within the restricted Hartree-Fock approximation, the UCC ansatz changes to only include pairs of electrons being removed from an occupied MO to a virtual MO. We therefore propose the following approximate ansatz unitary, for reaching an approximate groundstate to the problem Hamiltonian:

$$\hat{U}^{(R)} = \exp(\hat{T}^{(R)}) \quad (14)$$

$$\hat{T}^{(R)} = \sum_{i \in v, j \in o} t_{i,j}^{(R)} (\hat{b}_i^+ \hat{b}_j - \hat{b}_j^+ \hat{b}_i) \quad (15)$$

$$\hat{T}^{(Q)} = \sum_{p,q} t_{p,q}^{(R)} (\hat{\sigma}_p^+ \hat{\sigma}_q^- - \hat{\sigma}_p^- \hat{\sigma}_q^+) \quad (16)$$

$$= \sum_{p,q} \frac{t_{p,q}^{(R)}}{2} (\hat{\sigma}_p^X \hat{\sigma}_q^Y - \hat{\sigma}_p^Y \hat{\sigma}_q^X) \quad (17)$$

where  $\hat{U}^{(R)}$  represents the exact coupled cluster unitary,  $\hat{T}^{(R)}$  is the restricted coupled cluster operator, the superscript  $(R)$  denotes the electron-singlet restricted Hartree-Fock approximation, and we transform  $\hat{T}_s$  to a qubit-acting cluster operator  $\hat{T}^{(Q)}$  using transformation rule Eq. (6). From the form of the ansatz it is clear the unitary operation is particle and spin conserving. There are  $(N - n_e)n_e$  terms, where  $n_e$  is the

number of electron pairs in the system and  $N$  is the number of orbitals. We call this the restricted unitary coupled cluster (R-UCC) ansatz.

A first-order Trotterization of evolution over the qubit operator Eq. (17) is given by

$$\hat{U}^{(R)} = \exp(\hat{T}^{(Q)}) = \exp\left(\sum_{p,q} t_{p,q}^{(R)} (\hat{\sigma}_p^+ \hat{\sigma}_q^- - \hat{\sigma}_p^- \hat{\sigma}_q^+)\right) \quad (18)$$

$$\approx \prod_{p,q} \exp(t_{p,q}^{(R)} (\hat{\sigma}_p^+ \hat{\sigma}_q^- - \hat{\sigma}_p^- \hat{\sigma}_q^+)) \quad (19)$$

where each  $\exp(t_{p,q}^{(R)} (\hat{\sigma}_p^+ \hat{\sigma}_q^- - \hat{\sigma}_p^- \hat{\sigma}_q^+))$  can be implemented as a partial swap gate between qubits  $p$  and  $q$ . The order of applications of the product of unitaries in Eq. (19) matters and can be chosen optimally to minimize the Trotter error [22, 23].

In Figure 1 we show how the above unitary can be simulated in linear circuit depth on a quantum hardware device using a discrete set of pre-programmed unitary operations (or “gates”), which are subsequently variationally optimized to prepare an approximation to the ground state. The qubits are initialized in the  $|0\rangle$  state and the lowest  $n_e$  orbitals are populated via an X-gate. The R-UCC circuit is then executed. In Figure 1a we show the corresponding quantum circuit diagram for a single Trotter step (this can readily be extended to larger numbers of Trotter steps). In Figure 1b we detail the Singlet-State Simulation (SSS) operation (“gate”). The SSS-gates are partial-SWAP gates followed by a full-swap gate. The full-swap gate  $\text{SWAP}(i, j)$  swaps the logical qubit labels in order to bring every logical qubit which was occupied next to every other logical qubit which was not. In this way, excitations from every occupied orbital to every virtual orbital is simulated, in a minimal gate-depth of  $N$ , even on a linear chain of qubits (nearest-neighbor connectivity) [11].

## V. MEASURING THE ENERGY

After performing state preparation with a parametrized circuit (with parameters  $t_{p,q}^{(R)}$ ), one may calculate the energy of the prepared state in different ways: either one employs Quantum Phase Estimation methods [5, 20] (which yield arbitrarily good precision but have coherence requirements too stringent for current-era NISQ hardware) or one employs Hamiltonian averaging and variationally optimizes over the resulting energy expectation value. We here focus on the latter, an implementation of a Variational Quantum Eigensolver (VQE [7]), although the R-UCC ansatz may in general be applied in any simulation strategy involving quantum chemistry state preparation.

In the measurement phase, one can only measure individual sets of mutually commuting operators due to the fundamental limits imposed on measurement by the laws of quantum mechanics. In conventional UCCSD-VQE, this set scales in size as  $\mathcal{O}(N^4)$ , increasing the overall computation time, which may be brought down to an upper bound of  $\mathcal{O}(N^6)$  measurements for most realistic molecules in a Gaussian type orbital basis set (see Ref. [26]). However in the restricted method described in this paper, all Hamiltonian operators can be sorted into just 2 groups of mutually commuting sets of operators; if we assume only single-qubit rotations are used for diagonalizing the Pauli strings, there are just 3 unique tensor product bases (I, Z and ZZ terms, XX terms, and YY terms). This gives only constant overhead,  $\mathcal{O}(1)$ , in the overall complexity due to the measurement phase contribution, with a worst-case-scenario scaling upper bound of  $\mathcal{O}(N^4)$  measurements due to shot repetition requirements at fixed desired accuracy. The final total time scaling of R-UCC is then estimated to have a polynomial speedup over state-of-the-art quantum simulation protocols. In Figure 2 we detail the workflow for R-UCC-VQE, where input data refers to the SCF pre-calculated data about the molecule and ‘output data’ refers to the simulated ground state energy.

## VI. DEMONSTRATION OF THE METHOD

We now demonstrate the R-UCC-VQE method described above and illustrate the applicability and advantages of the restricted Hartree-Fock approximated simulation method by applying it to the ground state energy estimation of the lithium hydride molecule. The lithium hydride molecule has been studied extensively using even exact methods in conventional computational chemistry, while the ground state structure is more complicated at all bond lengths than simple molecules like dihydrogen and helium-hydride. As such, the Hartree-Fock state has insufficient overlap with the groundstate and a good ansatz operator is required to reach chemical accuracy with the exact ground state energy within a given basis. It therefore presents a challenging, yet exemplary test case for any near-term quantum computational chemistry algorithm.

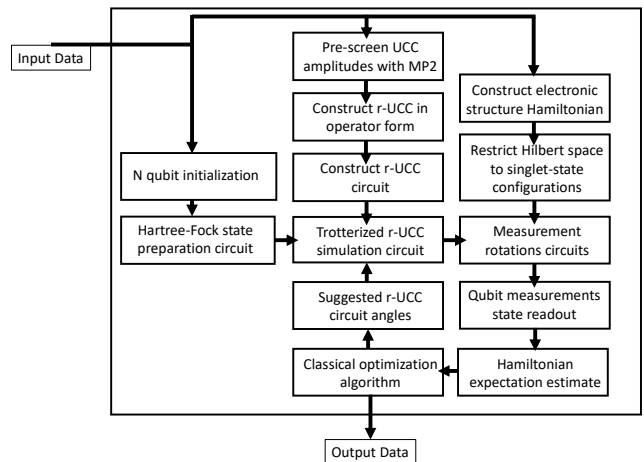


FIG. 2. Flowchart detailing the workflow when applying the restricted Hartree-Fock method on a quantum computer, specifically with a VQE treatment, a hybrid quantum-classical approach. The input data consists of the molecular chemistry data such as basis set, electron number, electron-electron integrals and more. The output data typically returns eigenenergies and convergence data of the classical optimization algorithm.

### A. Comparison of converged results without noise

We start with simulation results obtained via a noise free evolution on a quantum computer simulator. We are first interested only in the expressive power of the R-UCC ansatz and will concentrate on issues of convergence and learning of the parameters later. Therefore, we initialize the angles based on the CCSD amplitudes found with PySCF [14] and compute the energy by calculating the exact Hamiltonian expectation value based on the simulated circuit wavefunction. In the simulation we have access to the full wave function and therefore the resulting expectation value of the energy is not stochastic. We thus here do not consider the issue of how to optimally decompose the Hamiltonian into operators that can be measured on an actual device [27]. It should be noted however, that due to the lower number of non-commuting terms, also here the R-UCC method has advantages over the standard UCC method.

We then variationally optimize the parameters of the ansatz preparation circuit Figure 1 and thereby find the R-UCC energy, which is an upper bound to the true ground state energy (in the respective basis and level of approximation). We compare the obtained energy with the exact ground state energy obtained by FCI in the unrestricted subspace, and the ground state energy obtained by exact diagonalization of the Hamiltonian in the restricted subspace (which we denote as FCI and R-FCI respectively).

In Figure 3 we show the simulation results for the lithium hydride molecule at various interatomic distances. We compare the different basis sets STO-6G (6 MOs), 4-31G (11 MOs) for the UCC methods and include FCI results in the large cc-pVDZ basis set (19 MOs) as a reference. Simulations of the R-UCC yield very good correspondence to the ex-

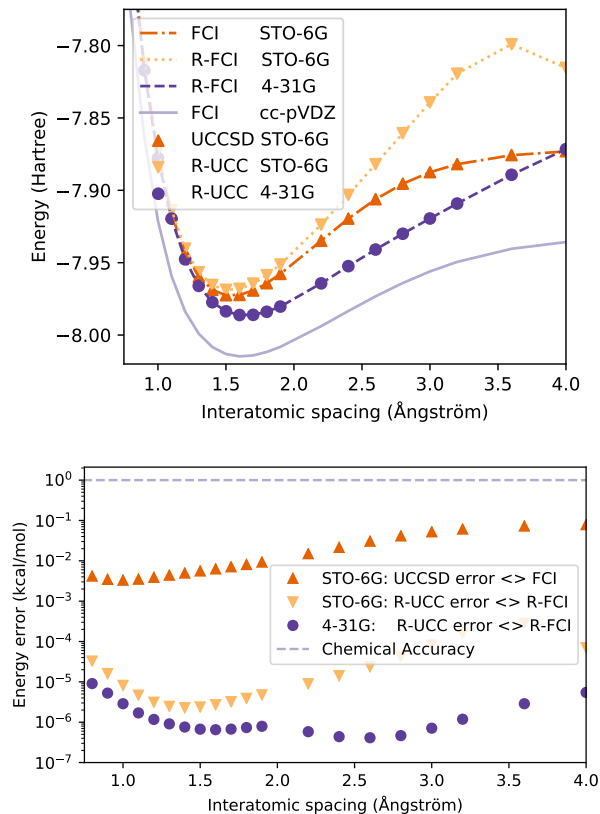


FIG. 3. (top) Ground state energy of the lithium hydride molecule as a function of interatomic distance. The light-purple (solid) curve depicts a highly accurate cc-pVDZ basis set FCI solution, the dark-orange (dash-dotted) curve depicts the FCI solution in STO-6G basis, the yellow (dotted) curve depicts the restricted-FCI solution in STO-6G basis, and the dark-purple (dashed) curve depicts the 4-31G basis restricted FCI solution. Dark-purple circles, dark-orange triangles and yellow triangles depict the R-UCC-VQE in 4-31G, UCCSD-VQE in STO-6G and R-UCC-VQE in STO-6G converged optimizer results, respectively. (bottom) Difference between converged R-UCC and R-FCI energies in the 4-31G and STO-6G basis sets, and difference between UCCSD and FCI energies in the STO-6G basis set, as a function of interatomic distance. Chemical accuracy is plotted for reference with a light-purple (dashed) line.

act ground state energy in the same basis set, over the whole range of interatomic distances.

When comparing our results to FCI results obtained from an unrestricted diagonalization in the much larger cc-pVDZ set, we find that the exact ground state energy in restricted 4-31G is much closer to cc-pVDZ, than that in the unrestricted basis STO-6G. The error introduced by the electron singlet approximation is much smaller than the error due to the smaller basis set. This is particularly noteworthy as the unrestricted STO-6G computation requires a comparable (and even slightly larger) number of qubits than the restricted 4-31G calculation (12 versus 11 qubits, respectively.) The additional error from using a single Trotter step VQE instead of FCI is well over a thousand times less than chemical accuracy (see Figure 3 bottom), which is the precision achieved typi-

cally in chemical experiments. All in all, we find that the R-UCC accuracy in the larger basis set is higher than the UCC accuracy in the smaller basis set, while at the same time requiring fewer quantum resources (11 instead of 12). We note that we have not applied any qubit reduction schemes, for example based on symmetries in the problem [28] or exploiting block-diagonality [29], but those same techniques can in principle also be used in the mapping used here.

## B. Convergence and training

We now compare the convergence of the R-UCC VQE optimization experiment with that of an (unrestricted) UCCSD-VQE. The R-UCC method requires fewer parameters for the classical optimizer to optimize over. This is because only the  $n_{occ} \times n_{virt}$  CC doubles amplitudes are to be considered within the restricted approximation. As in any CC technique, one may do MP2 pre-screening to reduce this number further.

So far we considered exact expectation values, but in practice one should consider the stochastic nature of Hamiltonian averaging process. The required number of shots is inversely proportional to the desired accuracy, squared. For the optimization of the VQE experiments, we set the number of shots such that the standard deviation was half of chemical accuracy, i.e.  $\frac{1}{2} \times 0.0016$  Hartree which is 0.5 kcal/mol. The statistics were estimated by a pre-calculation with the ansatz initialized at the CCSD angles setting for both the R-UCC and the UCCSD experiments, resulting in an estimated need of 41,000 and 100,000 shots respectively. We used the Implicit Filtering algorithm [30] for the classical optimizer to cope with the derivative-free, noisy blackbox function optimization.

The number of groups of commuting Pauli terms which share a tensor product basis, in the case of conventional UCCSD simulation is 182, while this number is just 3 for the R-UCC simulations.

In Figure 4 we plot the results for simulating LiH at equilibrium bond distance, showing the same three basis settings as in Figure 3). We find that: not only does the R-UCC method in the larger basis set (4-31G) converge to a lower final energy than the unrestricted UCCSD with a similar number of qubits in the smaller basis set (STO-6G), it also does so with nearly three orders of magnitude fewer total number of calls to the QPU (shots). Also during the training, the R-UCC method consistently gives better results for same number of shots. Given the gate and readout times of present and near future quantum computers, such reduction in the total number of quantum experiments can well be the decisive factor for whether a quantum simulation of a molecule is feasible or not.

Similarly, one may compare the convergence within the same basis set (STO-6G). Also here the number of calls to the QPU shrink by nearly three orders of magnitude, but the advantage of converging to a more precise final value is lost, at the advantage of a reduction in qubits needed.

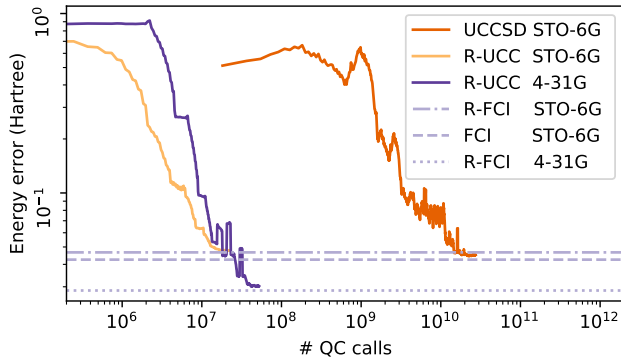


FIG. 4. Convergence of LiH groundstate energy simulation using three different VQE Coupled-Cluster implementations. The y-axis shows the energy error (in Hartree) with respect to the FCI groundstate energy in cc-pVDZ basis. The curves represent the overall convergence behaviour of VQE experiments for UCCSD in STO-6G, R-UCC in STO-6G and R-UCC in 4-31G (dark-orange, yellow and dark-purple curves, respectively). The plotted curves are averaged over 10 runs and a 10-point smoothing window is convoluted with it to suppress fluctuations and make the overall behavior more apparent. The x-axis expresses the total number of times the quantum circuit is initialized, run and measured. As reference lines, we plot the exact FCI and R-FCI groundstate energies in each respective basis in light-purple (dash-dotted, dashed, and dotted curves).

### C. Influence of noise

In NISQ-era devices, noise has a significant detrimental impact on the accuracy of computations. We note that in the above simulations the circuit was executed perfectly without noise or errors, and the energy estimation was taken over the exact wave function. Although a full consideration of the noise goes beyond the scope of this work, we may compare R-UCC to conventional UCCSD, where the R-UCC method has a much smaller total gate count and (two-qubit) circuit depth. This reduces the influence of decoherence and increases overall fidelity, which means that the R-UCC results should be more robust against noise than UCC.

Many noise mitigation techniques beyond VQE’s inherent error suppression have been proposed, such as noise extrapolation techniques, probabilistic error cancellation, quantum subspace expansion, stabilizer based methods and more (for a recent overview, please see f.ex. [13]). All these can be used in the present R-UCC-VQE method as well. In particular the stabilizer method would entail doing parity checks on the number of electron pairs which is a conserved quantity according to the electronic structure Hamiltonian. Also, all Hamiltonian term measurements which are done in the Z-basis (which is a significant portion of the total sets of measurements (1/3)) can natively be used to check the electron number without additional circuits.

### D. Beyond VQE

Regarding the computational scaling of quantum algorithms in general, beyond VQE, a similar argument as above can be made using a restricted-Hilbert space approach.

In conventional quantum phase estimation (QPE) (we refer the reader to Ref. [3] for a short review of the different versions of the QPE algorithms), an ancillary qubit register is added to the quantum circuit which aids in measuring eigenenergies of the Hamiltonian operator in  $\mathcal{O}(1)$  measurements and  $\mathcal{O}(1/\epsilon)$  circuit depth, given a trial state preparation with a significant overlap to the eigenstate of interest. For some systems, it has been proven that the HF-state, a simple product state preparable using  $\mathcal{O}(1)$  gates, may have exponentially vanishing overlap with the true ground state. In that case, a better state preparation scheme such as UCC or R-UCC is advantageous. In either of these cases, the scaling is improved, because R-UCC state preparation has only  $\mathcal{O}(N)$  depth and adiabatic state preparation at most  $\mathcal{O}(N^2)$  assuming parallelizable gate operations.

Further, in the phase estimation part of QPE, the controlled unitaries describing the Hamiltonian evolution require a gate depth scaling at most as  $\mathcal{O}(N^3)$  ( $N^2$  terms in the Hamiltonian, requiring at most  $N$  operations per term) per Trotter step. This is much less than in the conventional unrestricted case with  $\mathcal{O}(N^5)$  operations ( $N^4$  terms in the Hamiltonian, requiring at most  $N$  operations per term) per Trotter step. These controlled-unitary gate operations are often challenging to realize practically on quantum devices, as they involve multi-qubit interactions which are hard to implement coherently. In the un-restricted Hamiltonian QPE simulation, these controlled-unitaries involve at most 5-qubit interactions whereas in the restricted Hamiltonian QPE the controlled-unitary operations can be performed with 3-qubit interactions. While both cases can be decomposed to two-qubit gate sequences, the complexity of this decomposition is drastically reduced.

The performance enhancement is likewise expected for Kitaev’s PEA and Iterative Phase Estimation methods, as the state preparation and controlled-unitary operations remain the main components contributing to the total runtime of the algorithms.

## VII. SUMMARY & OUTLOOK

We have proposed a quantum algorithm for simulating molecular chemistry leveraging the restricted approximation to reduce the required quantum resources. The quantum circuit depth of our restricted unitary coupled cluster (R-UCC) circuit scales linearly with the number of molecular orbitals (MOs)  $N$ , a significant improvement over conventional UCCSD circuit depth, allowing the implementation on near-term quantum devices. Additionally, while conventional un-restricted second-quantized Hamiltonians have  $\mathcal{O}(N^3) - \mathcal{O}(N^4)$  (depending on optimal sorting capabilities) sets of Hamiltonian terms which can be measured simultaneously using only single-qubit rotations for the basis changes,

our restricted Hamiltonian scheme has just  $N^2$  terms, which can be sorted into just 3 sets of terms which can be measured simultaneously with SQB basis changes. This results in a drastic improvement in the number of runs necessary for Hamiltonian averaging and thereby of the overall quantum computing time. Additionally, the number of free parameters to be optimized by the classical optimizer is reduced considerably, as only pair-excitations are considered in the ansatz circuit. The R-UCC protocol enables efficient use of a parallelized circuit for Trotterized ansatz simulation with only native two-qubit gate requirements, such that the qubit lattice connectivity requirement is relaxed compared to previous UCC proposals. Only a single linear chain needs to be defined across the lattice to reach the provably minimal linear gate depth shown in [11]. Restricting the subspace to only include superpositions of electron singlet-configurations also allows for quantum phase estimation to be implemented more efficiently. In this way, also fault tolerant quantum computers devices may profit from a increase in computational accuracy enabled by spending freed up quantum computing resources on a larger basis set. We note that the only required unitary operations in R-UCC are single-qubit rotations and the SSS gate, which is a partial-swap operation. Specialized quantum hardware may implement such a two-body partial-swap far more efficiently than conventional generalized universal-gate quantum computing hardware. We also note that the restricted approximation works rather well for nuclear geometries close to the equilibrium. Indeed, in Figure 3 the R-UCC and FCI curves go parallel below an interatomic distance of 3.0 Å. That reinforces the validity of the restricted approximation in geometries close to equilibrium where no electronic radicals are present.

To conclude, the molecular chemistry simulation scheme proposed here opens up new possibilities towards near-term quantum chemistry simulation in addition to presenting a promising outlook for optimal use of future large-scale fault tolerant quantum devices.

### Appendix A: Hamiltonian matrix elements

We here detail how the Hamiltonian matrix elements  $h_{p,q,r,s}$  are calculated from the electron-integrals, in the case

of both the Fermionic as well as for the Hard-Core Bosonic hamiltonians. The electron integrals calculated with [14] are stored in arrays of the form

$$\mathbf{e}_{\text{sei}} \quad (N \times N) \quad (\text{A1})$$

$$\mathbf{e}_{\text{tei}} \quad (N \times N \times N \times N) \quad (\text{A2})$$

where  $N$  is the number of Molecular Orbitals (2 electrons fit in each orbitals, so  $2N$  spin-orbitals in total).

The Fermionic Hamiltonian in second quantization and Born-Oppenheimer approximation is written as

$$\hat{H} = C + \sum_{p,q} h_{p,q} \hat{a}_p^\dagger \hat{a}_q + \frac{1}{2} \sum_{p,q,r,s} h_{p,q,r,s} \hat{a}_p^\dagger \hat{a}_q^\dagger \hat{a}_r \hat{a}_s, \quad (\text{A3})$$

where indices  $\{p, q, r, s\}$  run from 1 to  $2N$ , where even indices indicate alpha electrons and odd indices are beta electrons. Then

$$h_{2i,2j} = h_{2i+1,2j+1} = \mathbf{e}_{\text{sei}}[i, j], \quad (\text{A4})$$

and

$$h_{2i,2j,2k,2l} = \mathbf{e}_{\text{tei}}[i, j, k, l] \quad (\text{A5})$$

$$h_{2i+1,2j+1,2k+1,2l+1} = \mathbf{e}_{\text{tei}}[i, j, k, l] \quad (\text{A6})$$

$$h_{2i,2j+1,2k+1,2l} = \mathbf{e}_{\text{tei}}[i, j, k, l] \quad (\text{A7})$$

$$h_{2i+1,2j,2k,2l+1} = \mathbf{e}_{\text{tei}}[i, j, k, l], \quad (\text{A8})$$

for indices  $i$  and  $j$  running from 1 to  $N$ . while the restricted-Hartree-Fock, or HCB, Hamiltonian can be written as

$$\hat{H}_r = C + \sum_{p,q} h_{p,q}^{(r1)} \hat{b}_p^\dagger \hat{b}_q + \sum_{p \neq q} h_{p,q}^{(r2)} \hat{b}_p^\dagger \hat{b}_p \hat{b}_q^\dagger \hat{b}_q, \quad (\text{A9})$$

where

$$h_{i,i}^{(r1)} = 2\mathbf{e}_{\text{oei}}[i, i] + \mathbf{e}_{\text{tei}}[i, i, i, i] \quad (\text{A10})$$

$$h_{i,j}^{(r1)} = \mathbf{e}_{\text{tei}}[i, i, j, j] \quad (i \neq j) \quad (\text{A11})$$

$$h_{i,j}^{(r2)} = 2\mathbf{e}_{\text{tei}}[i, j, j, i] - \mathbf{e}_{\text{tei}}[i, j, i, j] \quad (i \neq j) \quad (\text{A12})$$

for indices  $i$  and  $j$  running from 1 to  $N$ .

[1] “Smulating physics with computers. keynote address delivered at the mit physics of computation conference,” (1982).  
 [2] C. Nay, “Ibm opens quantum computation center in new york; brings world’s largest fleet of quantum computing systems online, unveils new 53-qubit quantum system for broad use,” IBM website (2019).  
 [3] Y. Cao, J. Romero, J. P. Olson, M. Degroote, P. D. Johnson, M. Kieferov, I. D. Kivlichan, T. Menke, B. Peropadre, N. P. D. Sawaya, S. Sim, L. Veis, and A. Aspuru-Guzik, *Chemical Reviews* **119**, 10856 (2019), pMID: 31469277, <https://doi.org/10.1021/acs.chemrev.8b00803>.  
 [4] J. Preskill, *Quantum* **2**, 79 (2018).

[5] A. Y. Kitaev, “Quantum measurements and the abelian stabilizer problem,” (1995), arXiv:quant-ph/9511026 [quant-ph].  
 [6] A. Aspuru-Guzik, A. D. Dutoi, P. J. Love, and M. Head-Gordon, *Science* **309**, 1704 (2005), <https://science.sciencemag.org/content/309/5741/1704.full.pdf>.  
 [7] A. Peruzzo, J. McClean, P. Shadbolt, M.-H. Yung, X.-Q. Zhou, P. J. Love, A. Aspuru-Guzik, and J. L. OBrien, *Nature Communications* **5**, 4213 (2014).  
 [8] T. Helgaker, P. Jorgensen, and J. Olsen, *Molecular Electronic-structure Theory* (Wiley, 2008).  
 [9] J. R. McClean, J. Romero, R. Babbush, and A. Aspuru-Guzik, *New Journal of Physics* **18**, 023023 (2016).

- [10] R. Babbush, N. Wiebe, J. McClean, J. McClain, H. Neven, and G. K.-L. Chan, *Phys. Rev. X* **8**, 011044 (2018).
- [11] I. D. Kivlichan, J. McClean, N. Wiebe, C. Gidney, A. Aspuru-Guzik, G. K.-L. Chan, and R. Babbush, *Phys. Rev. Lett.* **120**, 110501 (2018).
- [12] J. Lee, W. J. Huggins, M. Head-Gordon, and K. B. Whaley, *Journal of Chemical Theory and Computation* **15**, 311 (2019), <https://doi.org/10.1021/acs.jctc.8b01004>.
- [13] S. McArdle, S. Endo, A. Aspuru-Guzik, S. Benjamin, and X. Yuan, “Quantum computational chemistry,” (2018), arXiv:1808.10402 [quant-ph].
- [14] Q. Sun, T. C. Berkelbach, N. S. Blunt, G. H. Booth, S. Guo, Z. Li, J. Liu, J. D. McClain, E. R. Sayfutyarova, S. Sharma, S. Wouters, and G. K. Chan, “Pyscf: the pythonbased simulations of chemistry framework,” (2017), <https://onlinelibrary.wiley.com/doi/pdf/10.1002/wcms.1340>.
- [15] P. Jordan and E. Wigner, *Zeitschrift für Physik* **47**, 631 (1928).
- [16] F. Jensen, *Introduction to Computational Chemistry* (John Wiley & Sons, Inc., Hoboken, NJ, USA, 2006).
- [17] N. Thang and P. Nga, *Communications in Physics* **21**, 301 (2011).
- [18] O. Bratteli and D. Robinson, *Operator Algebras and Quantum Statistical Mechanics: Equilibrium States. Models in Quantum Statistical Mechanics*, Theoretical and Mathematical Physics (Springer Berlin Heidelberg, 2003).
- [19] R. J. Bartlett, S. A. Kucharski, and J. Noga, *Chemical Physics Letters* **155**, 133 (1989).
- [20] M. A. Nielsen and I. L. Chuang, *Quantum Computation and Quantum Information: 10th Anniversary Edition* (Cambridge University Press, 2010).
- [21] M. Suzuki, *Physics Letters A* **146**, 319 (1990).
- [22] H. R. Grimsley, D. Claudino, S. E. Economou, E. Barnes, and N. J. Mayhall, arXiv **arXiv** (2019), arXiv:1910.10329v1.
- [23] A. Tranter, P. J. Love, F. Mintert, N. Wiebe, and P. V. Coveney, *Entropy* **21**, 1218 (2019).
- [24] P. K. Barkoutsos, J. F. Gonthier, I. Sokolov, N. Moll, G. Salis, A. Fuhrer, M. Ganzhorn, D. J. Egger, M. Troyer, A. Mezzacapo, S. Filipp, and I. Tavernelli, *Phys. Rev. A* **98**, 022322 (2018).
- [25] P. J. J. O’Malley, R. Babbush, I. D. Kivlichan, J. Romero, J. R. McClean, R. Barends, J. Kelly, P. Roushan, A. Tranter, N. Ding, B. Campbell, Y. Chen, Z. Chen, B. Chiaro, A. Dunsworth, A. G. Fowler, E. Jeffrey, E. Lucero, A. Megrant, J. Y. Mutus, M. Neeley, C. Neill, C. Quintana, D. Sank, A. Vainsencher, J. Wenner, T. C. White, P. V. Coveney, P. J. Love, H. Neven, A. Aspuru-Guzik, and J. M. Martinis, *Phys. Rev. X* **6**, 031007 (2016).
- [26] J. R. McClean, R. Babbush, P. J. Love, and A. Aspuru-Guzik, *The Journal of Physical Chemistry Letters* **5**, 4368 (2014), pMID: 26273989, <https://doi.org/10.1021/jz501649m>.
- [27] W. Huggins, J. McClean, N. Rubin, Z. Jiang, N. Wiebe, K. Whaley, and R. Babbush, (2019), arXiv:1907.13117.
- [28] S. Bravyi, J. M. Gambetta, A. Mezzacapo, and K. Temme, “Tapering off qubits to simulate fermionic hamiltonians,” (2017), arXiv:1701.08213 [quant-ph].
- [29] N. Moll, A. Fuhrer, P. Staar, and I. Tavernelli, *Journal of Physics A: Mathematical and Theoretical* **49**, 295301 (2016).
- [30] C. T. Kelley, *Implicit Filtering* (Society for Industrial and Applied Mathematics, 2011) <https://epubs.siam.org/doi/pdf/10.1137/1.9781611971903>.